nature neuroscience

UNC-6/Netrin induces neuronal asymmetry and defines the site of axon formation

Carolyn E Adler, Richard D Fetter & Cornelia I Bargmann

UNC-6/Netrin and its receptor UNC-40/DCC are conserved regulators of growth cone guidance. By directly observing developing neurons *in vivo,* we show that UNC-6 and UNC-40 also function during axon formation to initiate, maintain and orient asymmetric neuronal growth. The immature HSN neuron of *Caenorhabditis elegans* breaks spherical symmetry to extend a leading edge toward ventral UNC-6. In *unc-6* and *unc-40* mutants, leading edge formation fails, the cell remains symmetrical until late in development and the axon that eventually forms is misguided. Thus netrin has two activities: one that breaks neuronal symmetry and one that guides the future axon. As the axon forms, UNC-6, UNC-40 and the lipid modulators AGE-1/phosphoinositide 3-kinase (PI3K) and DAF-18/PTEN drive the actin-regulatory pleckstrin homology (PH) domain protein MIG-10/lamellipodin ventrally in HSN to promote asymmetric growth. The coupling of a directional netrin cue to sustained asymmetric growth via PI3K signaling is reminiscent of polarization in chemotaxing cells.

Early in its development, a neuron extends long neurites tipped by dynamic, actin-rich growth cones. These neurites may become axons or dendrites, depending on the activity of an intrinsic neuronal polarity program that is regulated by the cytoskeleton, PAR polarity proteins, and lipid and protein kinases[1–7]. Although the ability to form long neurites is a defining feature of neurons, it is unclear what causes a neuron to break spherical symmetry and elongate processes. Studies *in vitro* have suggested that symmetry breaking is an active process that can be stimulated by neurotrophins or extracellular matrix components[6,8], but little is known about the mechanisms that initiate and orient asymmetric growth *in vivo*[7].

Scattered studies of axonogenesis *in vivo* suggest that neurons usually extend their first stable process in the exact direction that will be taken by the eventual axon. Both the initial exploratory filopodia and the first microtubule-containing process of the grasshopper Ti1 neuron emerge from the cell body in the direction of its future axon[9]. Developing vertebrate retinal ganglion cells (RGCs) send their axons directly toward the optic nerve head, a trajectory marked before the growth cone forms by a small thickening of the RGC membrane[10]. These observations suggest that guidance information might direct the earliest stage of asymmetric neuronal growth.

Axon formation has conceptual similarities to the polarization of cells during chemotaxis[11,12]. In both cases, a symmetrical cell generates an asymmetric domain, the growth cone or leading edge, that guides further motility. In chemotaxing cells, chemoattractants recognized by G protein–coupled receptors trigger both the onset of asymmetry and directed cell movement. Lipid products of the PI3K localize to the future leading edge and can organize leading edge formation[13]. Cell asymmetry does not require graded external signals: a uniform pulse of chemoattractant leads to the all-or-none creation of a single leading edge, amplifying a random initial asymmetry into a strongly polarized intracellular response[11].

The secreted UNC-6/netrin proteins function in axon guidance and cell migration in both vertebrates and invertebrates[14–17]. Netrins can attract or repel migrating cells and axons. The UNC-40/DCC family of receptors mediates attraction to netrin in most circumstances[18,19], whereas the UNC-5 family of receptors mediates repulsion from netrin[20]. In the nematode *C. elegans*, UNC-6 is secreted by neurons of the ventral nerve cord, and neurons expressing UNC-40 send axons ventrally toward it[14,15]. In particular, the HSN motor neurons are guided ventrally by strong attraction to UNC-6 (ref. 21).

Here we describe the early development of the HSN neuron as it generates a growth cone *in vivo*. We show that UNC-6/netrin and its receptor UNC-40/DCC have an unexpectedly early role in generating, maintaining and orienting asymmetric growth before axon formation. The conserved actin regulator UNC-34/Enabled, the PH domain protein MIG-10/lamellipodin and lipid signaling direct axon formation in response to UNC-6/netrin. Our results suggest that netrin drives neuronal growth through mechanisms that parallel leading edge formation.

RESULTS

Characterization of wild-type HSN development

Each of the two bilaterally symmetric HSN neurons sends a single axon ventrally to the ventral nerve cord, where the axon turns anteriorly and grows to the head (**Fig. 1a**,**b**). HSN axons extend during postembryonic stages, facilitating the analysis of their development[22]. We expressed a myristoylated green fluorescent protein (myr-GFP) marker selectively

Howard Hughes Medical Institute, Laboratory of Neural Circuits and Behavior, Rockefeller University, 1230 York Avenue, New York, New York 10021, USA. Correspondence should be addressed to C.I.B. (cori@rockefeller.edu).

Received 27 December 2005; accepted 14 February 2006; published online 5 March 2006; doi:10.1038/nn1666

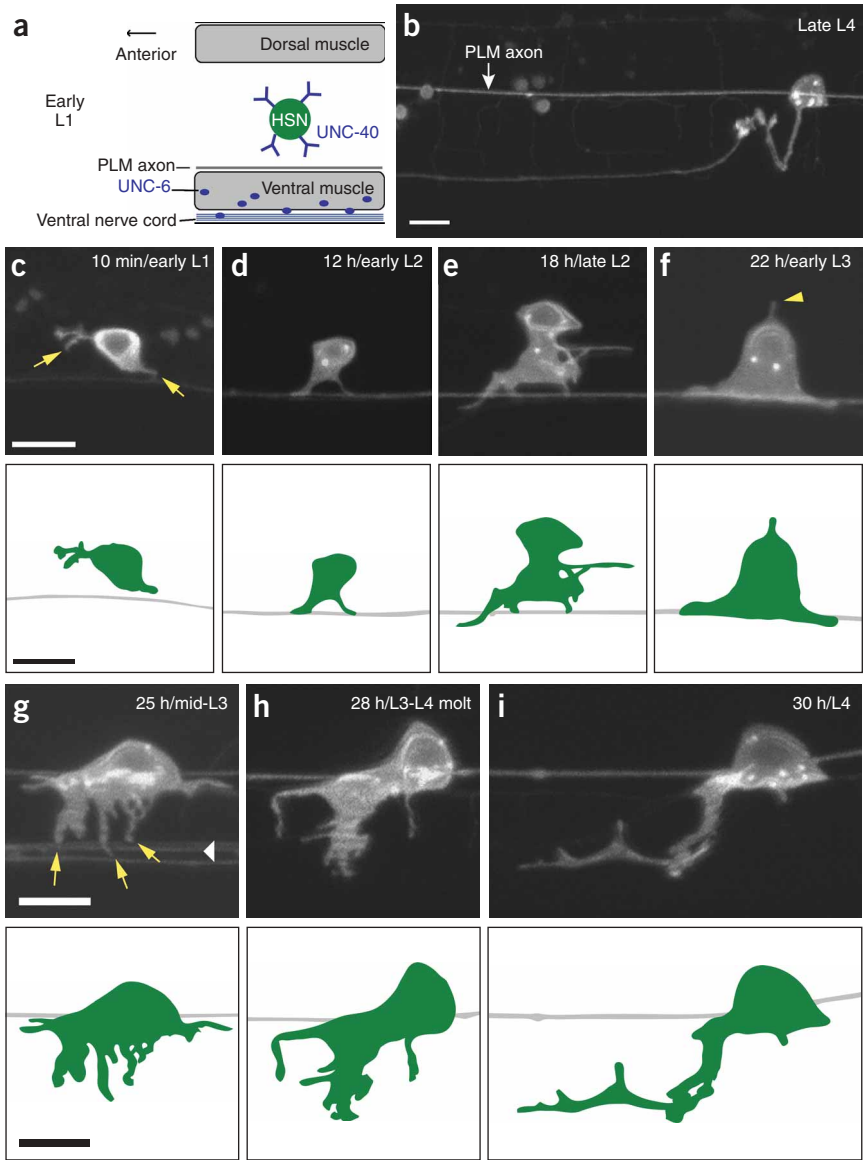

Figure 1 Development of HSN in wild-type *C. elegans*. (**a**) HSN expresses UNC-40/DCC receptors, which guide the axon towards UNC-6/netrin in the ventral nerve cord (VNC). (**b**) Mature HSN, late L4 stage. Axon extends ventrally, then anteriorly, and defasciculates from the VNC to form synapses at the vulva. (**c**–**i**) Lateral views of HSN in wild-type larvae expressing *unc-86::myr-GFP*, paired with schematic diagrams. Green, HSN; gray, PLM axon, which also expresses *unc-86::myr-GFP*. Hours of development and developmental stage are noted. (**c**) Early L1. HSN extends filopodia in random directions (arrows). (**d**) Early L2. HSN is polarized ventrally. (**e**) Late L2. Ventral side of HSN has a dynamic leading edge. (**f**) Early L3. HSN cell body has migrated ventrally, leaving a dorsal retraction fiber (arrowhead). (**g**) Mid-L3. HSN extends multiple neurites (arrows) toward the VNC (arrowhead). (**h**) L3-L4 transition. One growth cone expands in size and the others retract. (**i**) Mid-L4. The growth cone has turned anteriorly after reaching the VNC. In all pictures, ventral is down and anterior is to the left. Scale bars: 10 μm in **b**; 5 μm in **c**–**i**.

in HSN in order to observe filopodia and other membrane-rich structures, and used this marker to investigate HSN axon guidance in synchronized larvae at defined developmental stages (Methods).

Immediately after hatching, HSNs extended short neurites in random directions from the cell body (**Fig. 1c**). Within 4 h, these neurites were primarily restricted to the ventral side of the cell (**Fig. 1d** and see below). For the next 12–18 h of the L1 and L2 larval stages, the ventral cytoplasm of HSN steadily increased in size, developing into a dynamic leading edge (**Fig. 1e**). The HSN cell body then migrated ~5 μm ventrally to its final position, leaving a transient dorsal extension that probably represents a retraction fiber from the migration (**Fig. 1f**). About 25 h after hatching in the mid-L3 stage, the HSN showed a burst of dynamics in which it extended multiple ventrally directed neurites from its cell body (**Fig. 1g**; 98% of HSNs extended neurites ventrally, $n = 109$). We observed filopodia extending and retracting from the leading edge of these neurites in time-lapse images (data not shown), suggesting that these are dynamic growth cones. When these neurites reached the ventral midline, one expanded in volume and the others disappeared (**Fig. 1h,i**). More than 24 h passed between the initial ventral polarization of the HSN and the formation of a single ventral axon.

The features of *C. elegans* growth cones have only been examined in a few cases, invariably after the initial formation of an axon[23]. Therefore, we examined ultrastructural features of nascent HSN neurites in serial-section electron micrographs of mid-L3 stage HSNs with multiple neurites and of L3-L4 transition HSNs in which a single axon had been selected (**Fig. 2a,b** and Methods). In the mid-L3 stage, each of the multiple HSN neurites had a few microtubules in its shaft and fine filaments in the distal neurite; in the L3-L4 stage, the single neurite had a microtubule-rich shaft and similar filaments in the distal neurite (**Fig. 2c–f**). It is likely that the fine filaments were F-actin, because a GFP-actin fusion protein was enriched in distal neurites (**Fig. 2g,h**). Neurites from *C. elegans* of both stages also contained many ribosomes (**Fig. 2e,f**). The main distinction between the multiple neurites at mid-L3 and the single axon at the L3-L4 boundary was a larger number of microtubules in the single axon shaft.

Netrin promotes leading edge formation

In *unc-6*– and *unc-40*–null mutants, the HSN axon grows anteriorly instead of ventrally[14,21]. To understand how the defect in ventral guidance arises, we examined the individual steps of HSN development in *unc-6*– and *unc-40*–null mutants. These experiments revealed unexpected defects in the asymmetric growth of HSN before the expected guidance defect.

At hatching, *unc-6* and *unc-40* HSNs generated small filopodia, like wild-type HSNs. In the wild type, neurites were soon restricted ventrally, both through the formation of new ventral neurites and through the elimination of neurites with different orientations (**Fig. 3a**); the ventral neurites expanded into the ventral leading edge. In *unc-6* and *unc-40*, the filopodia did not develop a ventral bias, nor did they coalesce to form a leading edge at any time during the L1 and L2 larval stages (**Fig. 3b,c**). Instead, the filopodia retracted and the

HSN cytoplasm expanded symmetrically (**Fig. 3d–f**). These results suggest that UNC-6 and UNC-40 are required for the formation of an asymmetric leading edge in HSN.

During the L3 stage, both wild-type and mutant HSNs showed a burst of neurite formation and filopodial dynamics. In the wild type, these neurites were primarily restricted to the ventral side of HSN; however, in the *unc-6* and *unc-40* mutants, neurites extended in all directions from the cell body (**Fig. 3g–j**). Thus netrin confines neurite extension to the ventral side of HSN. Despite these defects, one primary growth cone was selected at the L4 stage at the same time as in the wild type (**Fig. 3k–n**). This result indicates that the timing of final HSN axon selection is independent of netrin and of interactions between HSN and specific targets in the ventral nerve cord.

Among molecules implicated in signaling downstream of UNC-40 are the Ena/vasodilator-stimulated phosphoprotein (VASP) protein UNC-34 (refs. 24–26; M. Dell & G. Garriga, personal communication), the Rac GTPase CED-10 (ref. 25), the actin-binding protein UNC-115 (ref. 25) and the actin-regulatory PH domain protein MIG-10/lamellipodin (refs. 27,28; C. Chang and C.I.B., unpublished results). Because of redundancy, single mutants in these genes have only mild defects in HSN ventral guidance, but some double mutants have highly penetrant defects in which most HSN axons grow laterally instead of ventrally[25] (C. Chang & C.I.B., unpublished results). A detailed analysis of HSN development revealed specialized roles of certain signaling proteins in asymmetric growth. In the L2 stage, *unc-34* and *mig-10* HSN neurons showed a symmetric, unpolarized morphology similar to that of *unc-6* and *unc-40* mutants (**Supplementary Fig. 1** online), implying that UNC-34 and MIG-10 are potential UNC-40 effectors in leading edge formation. Asymmetric growth was mostly unaffected by mutations in the Rac GTPase *ced-10*, the related GTPase *mig-2* or the actin-binding protein *unc-115/AbLIM* (**Supplementary Fig. 1**).

The HSN cell body did not migrate ventrally in *unc-6* and *unc-40* mutants, raising a concern that the ventral migration might be necessary for subsequent axon guidance. However, over 90% of *unc-34* HSN neurites grew ventrally in the L3 stage, even though *unc-34* mutants were highly defective in HSN cell migration (**Supplementary Fig. 1**). These results suggest that *unc-6* and *unc-40* are directly required both for ventral cell migration and for ventral axon guidance.

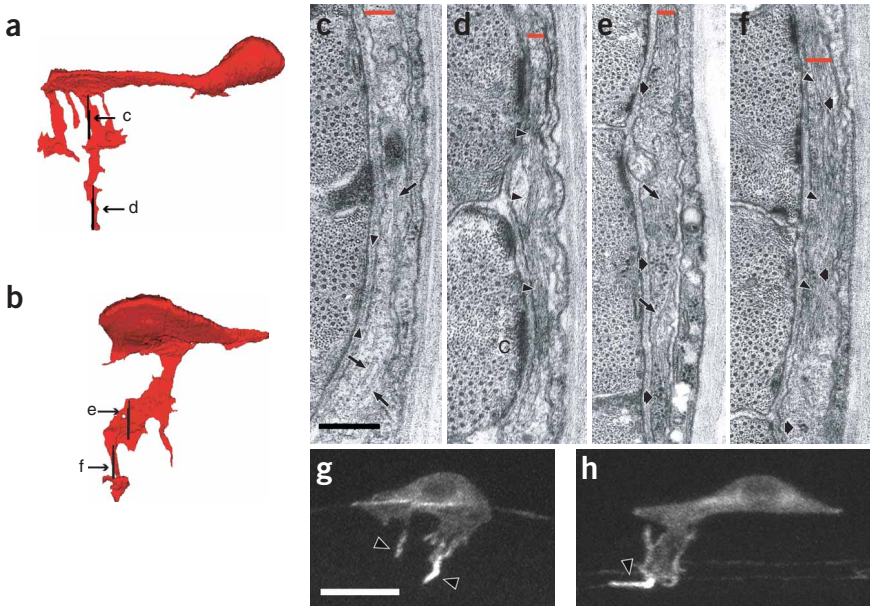

Figure 2 HSN neurites are microtubule-containing, actin-rich structures. (**a**,**b**) HSN reconstructions based on serial EM sections. (**a**) Mid-L3 HSN with multiple neurites. (**b**) L3-L4 transition HSN with a single axon. Anterior is to the left and ventral is down. (**c**–**f**) Electron micrographs of HSN neurites. The position and orientation of the micrographs are indicated by the labeled vertical lines in **a** and **b**. In each section, a red bar marks the position of the HSN neurite. From left to right, each section includes muscle, basement membrane, the HSN neurite, epidermis and cuticle. Medial is to the left and ventral is down. In **c** and **d**, cross-sections of a neurite from **a**. (**c**) Proximal region showing microtubules in tangential view (arrows). Arrowheads span a stretch of basement membrane. (**d**) Distal region enriched in filaments (arrowheads). In **e** and **f**, cross-sections of a neurite from **b**. (**e**) Proximal region containing microtubules in tangential view (arrows) and ribosomes (fat arrows). (**f**) Distal region enriched in filaments (arrowheads) and ribosomes (fat arrows). In **g** and **h**, HSN neurons expressing GFP-actin at mid-L3 (**g**) and L3-L4 transition (**h**). Fluorescence is enriched in the distal regions of the neurites (arrowheads). Anterior is to the left and ventral is down. Scale bars: 200 nm in **c**–**f**; 5 μm in **g**,**h**.

Netrin polarizes HSN acutely and continuously

To ask where and when netrin acts to regulate HSN development, we altered netrin expression using a hemagglutinin (HA)-tagged UNC-6 protein under the control of a heat shock promoter[29]. *unc-6;hs::unc-6::HA* transgenic nematodes grown at 15 °C did not express detectable protein but showed a substantial induction of UNC-6::HA expression after a 2-h heat shock at 30 °C (**Fig. 4a**). The induction of *hs::unc-6::HA* in the wild type during the L2 stage caused axon guidance errors in 25% of HSNs, suggesting that delocalized UNC-6::HA disrupts an instructive spatial pattern of netrin expression ($n = 102$) (**Fig. 4b**,**c**). Control experiments indicated that heat shock expanded UNC-6::HA expression outside its normal range: for example, heat shock disrupted the dorsal migration of the gonad arms, which are normally repelled from UNC-6 (33% of gonads misguided, $n = 100$) (**Fig. 4d**,**e**).

In *unc-6* mutants, HSN was symmetrical until the end of the L2 larval stage (**Fig. 3b**), a window of approximately 40 h at 15 °C. A 2-h heat shock applied either early (12 h) or late (24 h) in this interval resulted in a significant increase in the HSN neurons that had a well-defined leading edge (**Fig. 4f–h**). Leading edge formation in response to netrin was transient, peaking 8 h after the induction of UNC-6::HA and returning to baseline after 20 h (data not shown). This result suggests that netrin acts continuously during the L1 and L2 stages to induce and maintain the HSN leading edge. In *unc-40* mutants, there was no change in HSN morphology after the induction of UNC-6::HA (**Fig. 4h**), indicating that UNC-6 acts through the UNC-40 receptor.

Although heat shock expression of UNC-6::HA rescued leading edge formation, it did not rescue the HSN ventral guidance defect. As expected for delocalized expression from the heat shock promoter, the leading edges induced by UNC-6::HA were randomly oriented (for example, **Fig. 4g**). In *unc-6* mutants grown at 15 °C, 14% ($n = 104$) of HSN axons reached the ventral nerve cord; after a heat shock that rescued early asymmetric growth, only 24% ($n = 107$) of HSN axons grew ventrally. Thus, ubiquitous UNC-6::HA did not rescue ventral guidance

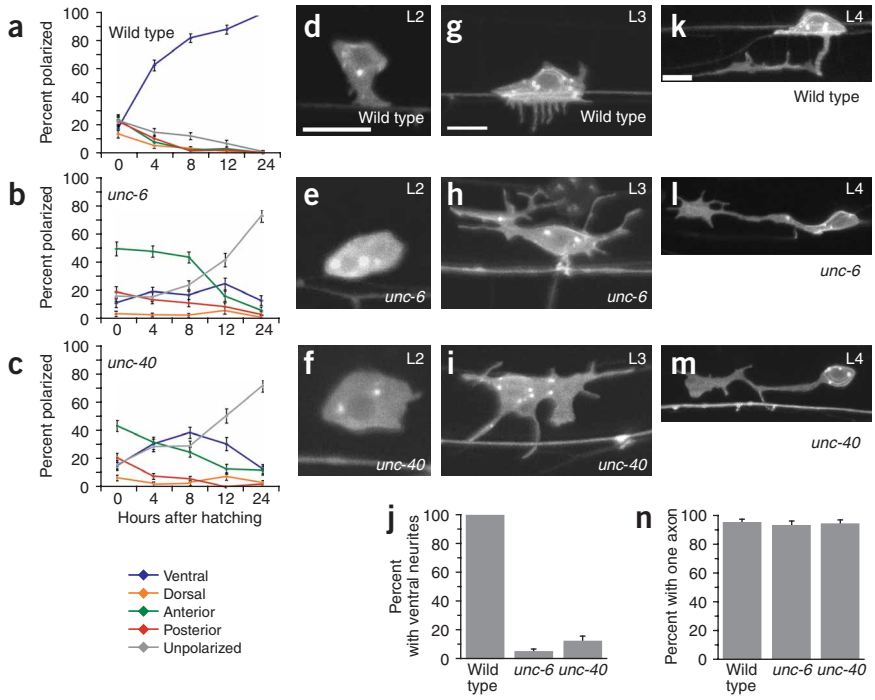

Figure 3 HSN development in netrin mutants. HSN development in wild-type, *unc-6(ev400)* and *unc-40(e271) C. elegans*. HSN was visualized with *unc-86::myr-GFP*. (**a**–**c**) Percentage of HSNs with filopodia or leading edges in the L1 and L2 stages. An HSN was scored as polarized if it had any filopodia or a leading edge, and the most prevalent direction of growth was noted. HSNs in *unc-6* and *unc-40* mutants had filopodia at early time points but did not form a leading edge at any time during this interval. (**d**–**f**) L2 stage HSNs. (**g**–**i**) L3 stage HSNs. (**j**) Percentage of HSN neurons with predominantly ventral neurites in mid-L3. (**k**–**m**) L4 stage HSNs. (**n**) Percentage of HSN neurons with a single axon in mid-L4. Error bars represent the standard error of proportion. For panels **a**–**c**, **j** and **n**, $n \geq 100$ cells. All images are lateral views with ventral down and anterior to the left. Scale bars, 5 μm.

in *unc-6* mutants and, moreover, disrupted ventral guidance in the wild type (**Fig. 4c**). These results indicate that UNC-6 provides both a general signal for HSN asymmetry and a spatial signal for axon guidance.

UNC-40 and MIG-10/lamellipodin are localized ventrally

GFP-tagged UNC-40 expressed from the *unc-86* promoter rescued polarized HSN growth and ventral HSN guidance in *unc-40* mutants (Methods), suggesting that *unc-40* functions cell-autonomously in HSN. In contrast with evenly distributed membrane markers like myr-GFP, the rescuing UNC-40::GFP protein became strongly localized to the ventral side of HSN beginning at the early L2 stage (**Fig 5a–f**). This result suggests that localization of signaling proteins in HSN accompanies leading edge formation and ventral growth.

To investigate this result further, we systematically examined HSN localization of numerous potential UNC-40 effectors including MIG-10, UNC-34 and CED-10. A rescuing MIG-10::yellow fluorescent protein (YFP) was markedly restricted to the ventral plasma membrane of HSN beginning at the late L2 stage (**Fig. 5g–i**). Functional GFP fusions to UNC-34 were enriched at the tips of filopodia but were present in both dorsal and ventral domains of the cell; functional GFP fusions to CED-10/Rac were dispersed across the entire HSN cell membrane (data not shown). Thus the ventral localization of UNC-40 and MIG-10 reflected protein-specific events in HSN during axon formation, not general cytoplasmic rearrangements.

MIG-10 localization requires netrin and lipid signaling

We used quantitative image analysis of staged *C. elegans* to determine the requirements for UNC-40::GFP and MIG-10::YFP localization in HSN. In wild-type L2 stage *C. elegans*, UNC-40::GFP intensity was twice as strong in the ventral HSN as in the dorsal HSN (**Fig. 5j**). In *unc-6* mutants, UNC-40::GFP was equally distributed across the HSN,

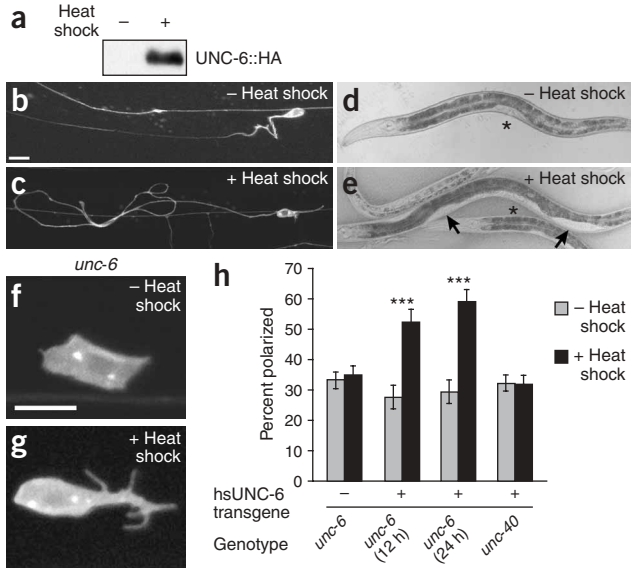

Figure 4 Heat-inducible expression of UNC-6/netrin induces leading edge formation in HSN. (**a**) Immunoblot with anti-HA antibody of *unc-6(ev400)* mutants expressing *hs::unc-6::HA*, raised at 15 °C (–) or exposed to heat shock at 30 °C for 2 h (+). (**b**,**c**) HSN in wild-type L4 larvae expressing *hs::unc-6::HA*. (**b**) Control L4 larva raised at 15 °C. (**c**) Heat shock causes axon wandering. (**d**,**e**) Gonads of wild-type L4 larvae expressing *hs::unc-6::HA*. (**d**) Control L4 larva raised at 15 °C. (**e**) Exposure to heat shock causes abnormal gonad morphology, marked by clear area (arrows). Asterisks indicate the developing vulva. (**f**,**g**) HSN in early L2 *unc-6* mutants expressing *hs::unc-6::HA*. (**f**) Control L2 larva raised at 15 °C, with unpolarized HSN morphology. (**g**) L2 larva exposed to 2 h heat shock during late L1 and examined in early L2. HSN has a polarized leading edge oriented in the wrong (posterior) direction. (**h**) Percentage of polarized HSNs after heat shock. A cell was scored as polarized if it had one leading edge (as in **g**) or if it had multiple filopodia oriented in one direction. $^{***}P < 0.001$ as determined by the *t*-test for proportions. For each condition, $n \geq 100$ cells. Error bars represent standard error of proportion. The polarization defect in *unc-6* and *unc-40* mutants was less severe here than in **Figure 3**, probably because the larvae were raised at 15 °C instead of 25 °C. In all pictures, anterior is to the left and ventral is down. Scale bars: 10 μm in **b** and **c**; 5 μm in **f** and **g**.

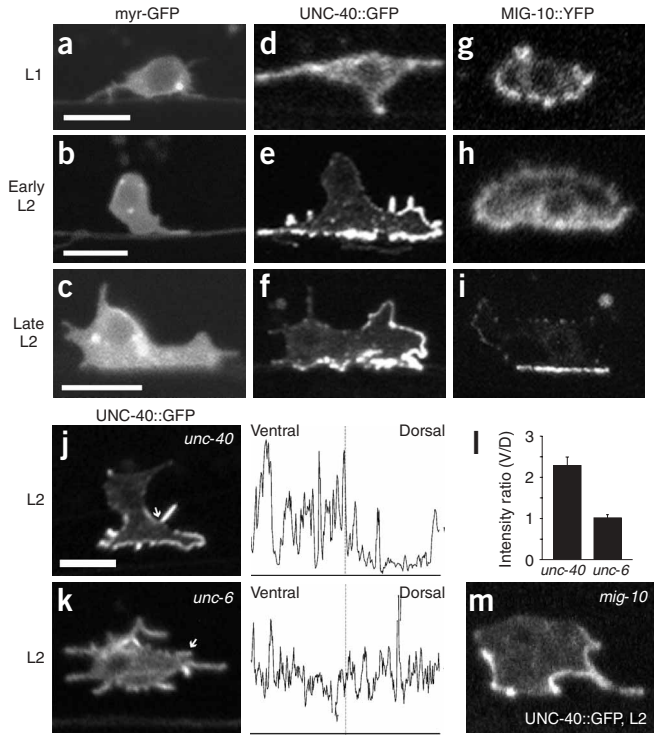

Figure 5 UNC-40::GFP and MIG-10::YFP are ventrally localized in HSN. (**a**–**c**) myr-GFP is evenly distributed in HSN membranes in the L1 and L2 stages. (**d**–**f**) UNC-40::GFP is preferentially localized to the ventral HSN in the L2 stage. (**g**–**i**) MIG-10::YFP is preferentially localized to the ventral HSN in the late L2 stage. (**j**–**k**) Lateral views of L2 stage HSNs expressing UNC-40::GFP. (**j**) *unc-40* mutant rescued by the *unc-40::GFP* transgene. (**k**) *unc-6* mutant. Traces are line-scan intensity plots (in arbitrary units) of the GFP signal around the periphery of the cell shown, starting from the arrow and moving clockwise. (**l**) Average ratio of dorsal to ventral intensity for >10 cells of each genotype. *unc-6* was statistically different from the control strain, a *unc-40* mutant rescued with the *unc-40::GFP* transgene ($P < 0.05$). Wild-type nematodes gave qualitatively similar results to rescued *unc-40* but were not quantified. Error bars indicate s.e.m. (**m**) UNC-40::GFP in *mig-10* mutant, same stage as in panels **j** and **k**. In all pictures, ventral is down and anterior is to the left. Scale bars, 5 μm.

indicating that netrin signaling is required for UNC-40 localization (**Fig. 5j–l**). In *mig-10* and *unc-34* mutants, UNC-40::GFP was enriched on the ventral side of the unpolarized HSN (**Fig. 5m** and data not shown). These results suggest that the ventral recruitment or clustering of UNC-40::GFP is an early response to UNC-6 signals that does not require MIG-10, UNC-34 or overt leading edge formation.

MIG-10::YFP intensity was more sharply localized than UNC-40::GFP, with a fourfold enrichment on the ventral HSN (**Fig. 6a**,**b**). Netrin signaling was essential for MIG-10::YFP localization, as MIG-10 was evenly dispersed across the cell membrane in *unc-6* and *unc-40* mutants (**Fig. 6c**,**d**). Moreover, disruption of the normal netrin pattern was sufficient to disrupt MIG-10::YFP localization in the wild type: the expression of *unc-6* from the dorsal muscle *unc-129* promoter caused dorsal MIG-10::YFP localization and dorsal HSN migration defects (Methods and **Supplementary Fig. 2** online). These results suggest that MIG-10 is localized by a spatial netrin cue and UNC-40 signaling. MIG-10 localization was unaffected in *unc-34* mutants, indicating that UNC-34 and leading edge formation are not required for ventral MIG-10 recruitment in HSN (**Fig. 6e**).

Members of the MIG-10/Riam/lamellipodin family contain a PH domain with specificity for phosphatidylinositol-3,4-bisphosphate ($PI(3,4)P_2$) phospholipids[28], which are generated by PI3K and destroyed by the phosphatase PTEN. To ask whether PIP_2 has a role in localizing MIG-10, we introduced MIG-10::YFP into a maternally rescued null mutant of *age-1*/PI3K and a null mutant of *daf-18*/PTEN (refs. 30,31; **Fig. 6f–h**). In *age-1* mutants, MIG-10::YFP was more weakly localized to the ventral side of HSN, based both on visual inspection and on quantitative measurements of protein distribution. MIG-10::YFP localization in *daf-18*/PTEN–null mutants was as defective as in netrin mutants. These results suggest that MIG-10::YFP localization requires PI3-containing phospholipids as well as netrin signaling.

During the L2 stage, *age-1* and *daf-18* mutants showed defects suggesting that lipid-dependent MIG-10 localization mediates leading edge formation. We found that 33% of *age-1* HSNs and 17% of *daf-18* HSNs were symmetric and unpolarized in the L2 stage, like *unc-6* mutant HSNs. A further 23% of the *daf-18* HSNs were polarized but in aberrant anterior, posterior or dorsal directions; *daf-18* mutants are predicted to have high levels of PI3 phospholipids, which could promote delocalized signaling. Thus, phospholipid signaling downstream of netrin promotes leading edge formation in HSN.

DISCUSSION

Our results indicate that the axon guidance factor UNC-6/netrin promotes, maintains and orients leading edge formation in the HSN neuron *in vivo*, stimulating axon formation as it guides the future axon. This process is associated with the asymmetric localization of the netrin receptor UNC-40 and the PH domain–containing protein MIG-10/lamellipodin.

Netrin orients HSN ventrally before growth cone formation

Previous experiments have demonstrated roles for netrin and its attractive receptor UNC-40/DCC in axon outgrowth and growth cone turning, but not in the earlier events that lead to axon formation[16,17]. By using a genetically encoded marker for a single neuron, we were able to visualize the entire process of axon formation directly; we found that netrin signaling promotes asymmetric neuronal growth and specifies the position at which the axon emerges from the cell.

Timely leading edge formation in HSN requires the activity of UNC-6 and its receptor UNC-40, as well as the cytoplasmic proteins UNC-34/Enabled and MIG-10/lamellipodin. Both loss-of-function and heat shock experiments indicated that netrin induces and maintains HSN asymmetry throughout the L1 and L2 stages of development. The cytoskeletal regulatory activities for leading edge formation could be provided by UNC-34/Ena and MIG-10/lamellipodin, as Ena/VASP stimulates actin-based filopodia formation and lamellipodin stimulates actin polymerization and lamellipodial extension[26,28].

The HSN eventually formed an axon in *unc-6* and *unc-40* mutants, but it was delayed and misguided. This axon grew anteriorly, the trajectory that HSN normally follows once it stops responding to netrin. It may be that other guidance factors—presumably those that promote anterior guidance—can stimulate asymmetric HSN growth at later times. We speculate that classical axon guidance factors could stimulate and orient asymmetric growth in many neurons. Indeed, semaphorin mutations alter the initial trajectory of vertebrate cortical axons[32], and the chemokine CXCR4, which blocks cellular responses to semaphorins and other repulsive guidance factors, affects the initial trajectory of some vertebrate motor axons[33]. Immature RGCs express the attractive netrin receptor DCC (ref. 34) and netrin-1 is expressed in

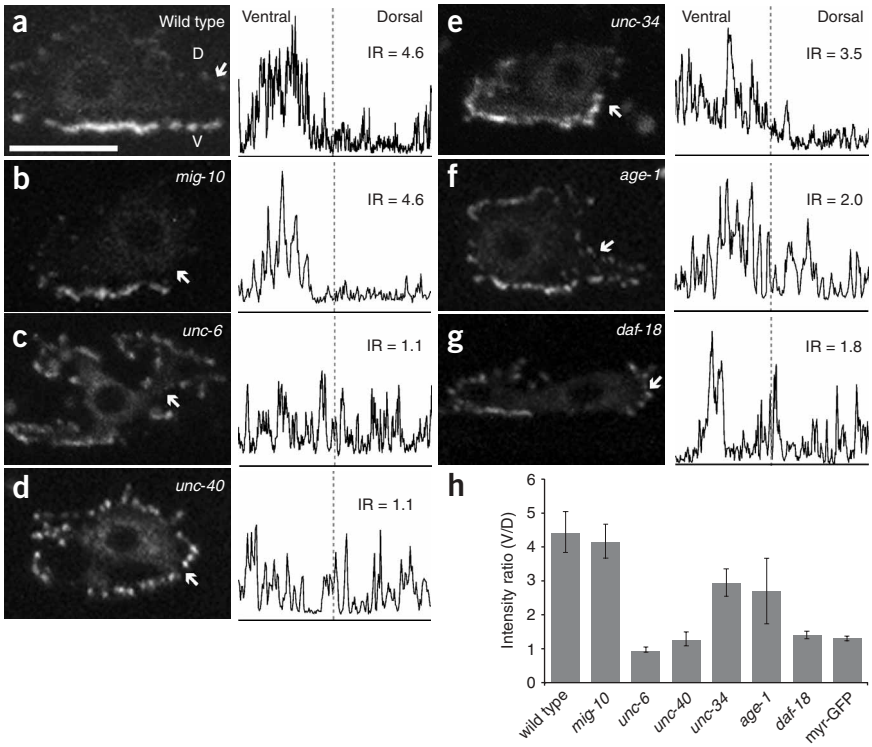

Figure 6 MIG-10::YFP localizes ventrally in a netrin-dependent manner. (**a**–**g**) Lateral views of L3 stage larvae expressing *unc-86::YFP::mig-10*. The HSN cell body fills most of each panel. Traces are line-scan intensity plots (in arbitrary units) of the YFP signal around the periphery of the cell shown, beginning at the arrow and moving clockwise. IR, intensity ratio. In **b**, *mig-10* mutant rescued by the *mig-10::YFP* transgene. (**h**) Average intensity ratios of MIG-10::YFP signals. Ratio was calculated as the intensity of the ventral half of the perimeter divided by the dorsal half ($n = 9$–14 cells for each genotype). The random distribution of myr-GFP in HSN is included as a control. Error bars indicate s.e.m. By Bonferroni *t*-tests ($P < 0.05$), wild type, *mig-10* and *unc-34* were indistinguishable; *unc-6, unc-40* and *daf-18* were highly defective; and *age-1* was intermediate. In all pictures, ventral is down and anterior is to the left. Scale bar, 5 μm.

the optic nerve head[35], suggesting that netrin could promote RGC polarization toward the nerve head.

Asymmetric MIG-10 and lipid signals mark the leading edge

Both the netrin receptor UNC-40 and the PH domain protein MIG-10 localized to the ventral side of HSN in response to UNC-6. The *Drosophila melanogaster* UNC-40 homolog Frazzled is also relocalized in response to netrin signaling, but unlike UNC-40, it does not follow the netrin distribution closely[36]. The sharp localization of MIG-10 is unique among the netrin effectors analyzed here or in other cell types. MIG-10 was not required for UNC-40 localization, but UNC-40 and asymmetric lipid signaling from PI3K and PTEN were required for the spatial restriction of MIG-10, suggesting that lipid signaling downstream of netrin creates the sharply localized front of MIG-10 at the ventral leading edge.

After a neuron breaks symmetry, its neurites are defined as axons or dendrites. Hippocampal axon-dendrite polarity is affected by PI3K activity[5,6,37]; PI3K products may link a neuron's ability to create a stable process with the specification of that process as the axon.

Lipid products of PI3K are implicated in the generation of a stable leading edge in neutrophils and *Dictyostelium discoideum* ameobae[11,12]. Our results suggest that PI3K-derived lipids have a similar function in HSN and that their target in HSN is MIG-10. The HSN defects in *age-1* and *daf-18* mutants were less severe than those in *mig-10* mutants, but this may have been due to residual lipid signaling. Although we used predicted null alleles, the *age-1* mutant is unlikely to eliminate all PI3K activity, both because of maternal rescue and because of the existence of a second unusual type-I PI3K in the *C. elegans* genome (F39B1.1).

In neutrophil chemotaxis, the first marker of cell asymmetry is the localization of PI3-containing lipids to one side of the cell; positive feedback between PI3K and Rac proteins then reinforces cell polarization[13]. During *Dictyostelium* chemotaxis, the localization of PI3K to the leading edge of the cell and that of the PI3 phosphatase PTEN to the trailing edge are required for polarized movement[38,39]. The analysis of HSN development suggests that polarized lipid signaling contributes to netrin-dependent axon formation and guidance. Pharmacological studies have demonstrated a requirement for PI3K in *Xenopus laevis* growth cone turning toward netrin-1, and the UNC-40 homolog DCC can bind directly to a phosphatidyl inositol transfer protein (PITP), suggesting that lipid signaling downstream of netrin is conserved in vertebrates and invertebrates[40–42].

METHODS

Strains and genetics. Wild-type nematodes were *C. elegans* variety Bristol, strain N2. Strains were maintained using standard methods[43]. The following mutations were used: *unc-40(e271, e1430)* I; *age-1(mg44)/mIn1[mIs14 dpy-10(e128)]* II; *mig-10(ct41)* III; *ced-10(n1993)* IV; *daf-18(nr2037)* IV; *unc-34(gm104, gm114, e315)* VL; *unc-6(ev400, e78)* X; *mig-2(mu28)* X; *unc-115(ky275)* X. Transgenic strains used were *kyIs262 [unc-86::myr-GFP; odr-1::DsRed]* IV; *kyIs299 [hsp16-2::unc-6::HA; unc-86::myr-GFP; odr-1::DsRed]* X; *kyEx710 [unc-86::GFP::unc-34; odr-1::DsRed]*; *kyEx682 [unc-86::GFP::actin; odr-1::DsRed]; kyEx926 [unc-86::mig-10::YFP; odr-1::DsRed]; kyEx1210* and *kyEx1211 [unc-86::unc-40::GFP; str-1::GFP]; kyEx1212 [unc-86::unc-40::GFP; odr-1::dsRed]*.

Germline transformation of *C. elegans* was performed as described[44] using *odr-1::dsRed* (25-50 ng μl^{-1}) and *str-1::GFP* (50 ng μl^{-1}) as coinjection markers.

The *unc-86::unc-40::GFP* transgene was scored for rescue of two HSN defects, ventral polarization and ventral axon guidance. Control *unc-40* nematodes had 12% polarized HSNs and 5% ventral HSN axons. Transgenic nematodes from one rescued line had 50% polarized HSNs and 55% ventral HSN axons, suggesting cell autonomous rescue; a second line gave comparable results.

Molecular biology. All plasmids for HSN expression contained a 5-kilobase fragment of the *unc-86* promoter[45]. Fusion genes included *myr-GFP*, in which the *C. elegans* Src myristoylation signal (GSCIGK) was inserted into the N terminus of GFP, a tagged *GFP::unc-34* cDNA, *GFP-actin* (gift from G. Seydoux, Johns Hopkins University, Baltimore), a tagged *mig-10::YFP* cDNA (gift from M. Krause, King's College London, London) and a tagged *unc-40::GFP* cDNA. An *unc-6* cDNA was cloned behind the dorsal muscle *unc-129* promoter to make *unc-129::unc-6* (ref. 46) and a tagged *HA::unc-6* cDNA (using pIM97; gift from B. Wadsworth, University of Medicine and Dentistry of New Jersey, Robert Wood Johnson Medical School, Piscataway, New Jersey)[15] was cloned behind the *hsp16-2* promoter to make *hsp16-2::unc-6::HA*. Details of plasmid construction are available upon request.

Developmental characterization of HSN. We observed HSN morphology mainly in anesthetized larvae from developmentally synchronized populations. The stages of HSN development described here are essentially synchronous in wild-type individuals.

Synchronized populations were obtained by allowing eggs to hatch overnight in M9 buffer without food; the resulting L1 nematodes were fed and grown at 25 °C to specified developmental stages. Control experiments indicated that starvation did not alter HSN development. Mutants were scored with respect to their developmental age rather than their age in hours, using gonad size (early and late L2, early L3), distal tip cell migration (mid-L3), and P6.p cell invagination (L3-L4 transition and mid-L4) as markers. **Figure 1c** depicts L1 larvae from eggs that were laid at 25 °C, allowed to hatch for 10 min, and examined immediately.

UNC-6 misexpression experiments. Nematodes expressing *hs::unc-6::HA* were grown to the specified stage at 15 °C, shifted to 30 °C for 2 h and recovered at 15 °C. HSN polarization was scored blindly after 8 h of recovery at 15 °C, when the maximum effect was observed.

To alter the spatial *unc-6* pattern more selectively, a full-length *unc-6* cDNA was expressed from the dorsal muscle *unc-129* promoter fragment[46]. *unc-129::unc-6* transgenes caused massive embryonic and larval lethality in wild-type and *unc-6* backgrounds, even when injected at low concentrations, and attempts to generate stable *unc-129::unc-6* transgenic lines were unsuccessful. We were able to obtain F1 transgenic nematodes after injection of the *unc-129::unc-6* transgene into the wild-type, but not *unc-6*, background. These transgenic F1s were identified based on the expression of a coinjected marker, *str-1::GFP*. HSN morphology and MIG-10 localization were scored in the L3 stage using MIG-10::YFP. In 8 of 52 F1 nematodes injected with *unc-129::unc-6*, the initial migration of the HSN was dorsal instead of ventral and the HSN cell body was located adjacent to dorsal muscles. This result suggests that dorsal *unc-129::unc-6* can override the normal ventral *unc-6* signal and guide HSN dorsally. All 8 of these nematodes showed dorsal localization of MIG-10::YFP instead of the normal ventral enrichment (**Supplementary Figure 2**). The 44 nematodes in which HSN migrated ventrally had ventral MIG-10::YFP, like the wild type. In control siblings lacking *unc-129::unc-6*, only 2 of 66 HSNs had dorsal MIG-10::YFP ($P < 0.05$) and none of the HSNs migrated dorsally. Expression of transgenes in F1 nematodes is typically incomplete or mosaic compared to the expression in stable transgenic lines; this mosaic expression would tend to minimize the gain-of-function effect of transgenes such as *unc-129::unc-6*. Therefore, the observed dorsal migration defects in 15% of HSNs represent a minimal estimate of the effects of dorsal *unc-6* expression.

Western blotting. *unc-6 kyIs299[hs::unc-6::HA]* nematodes were grown at 15 °C, shifted to 30 °C for 2 h, returned to 15 °C for 2 h and boiled in Laemmli buffer for SDS-polyacrylamide gel electrophoresis (SDS-PAGE). UNC-6-HA was detected with an antibody to HA (anti-HA; Roche Diagnostics).

Light microscopy and quantification. Nematodes were immobilized using 5 mM NaN_3 in 2% agarose. For standard imaging, populations of nematodes were examined on a Zeiss AxioplanII. Confocal images were taken on a Bio-Rad MRC1024 confocal with a 63× objective or a Zeiss LSM510. For quantification of the MIG-10::YFP and UNC-40::GFP signal, stacks were collapsed into a single image using the sum function in MetaMorph. A line was drawn around the cell periphery, and the linescan function was used to calculate the intensity at each point. To calculate the intensity ratio, the perimeter of each cell was divided into two equal lengths (ventral and dorsal), the background was subtracted from each pixel, and the intensity of the pixels along the line were added together.

Electron microscopy. Mid-L3 and L3-L4 transition *kyIs262* nematodes were prepared for electron microscopy by high pressure freezing using a Bal-Tec HPM 010 device followed by freeze-substitution using 1% OsO_4 and 0.1% uranyl acetate in 95% acetone and 5% methanol on dry ice, or with a Leica AFS freeze-substitution device. The substituted samples were embedded in Eponate 12 resin (Ted Pella), sectioned with a Leica Ultracut T ultramicrotome, stained with uranyl acetate and Sato's lead[47] and photographed using a JEOL 1200 EX/II operated at 80 kV. Reconstructions from serial section images were performed using the program Reconstruct (http://synapses.bu.edu).

Two L3 HSNs and a single L3-L4 HSN were reconstructed in their entirety from serial electromicrograph (EM) sections. Actin filaments, microtubules, ribosomes, Golgi stacks, basal bodies and vesicles were examined in each section for each cell. No basal bodies were visible in any HSN at this stage, although numerous basal bodies were visible in adjacent cells in the same sections. Each HSN had multiple Golgi stacks. In one L3 HSN, two Golgi stacks were on the ventral side and two were on the dorsal side. In the second L3 HSN, four Golgi stacks were on the ventral side and one was on the dorsal side. In the L3-L4 HSN, one Golgi stack was ventral, one was dorsal and three were lateral. Additional nematodes from both L3 and L3-L4 developmental stages were examined semiserially. Notable features of the reconstructed cells were also observed in the partial series.

Note: Supplementary information is available on the Nature Neuroscience website.

ACKNOWLEDGMENTS

We thank M. Krause, F. Gertler, M. Dell, G. Garriga and C. Chang for sharing results before publication; B. Wadsworth, Z. Gitai, T. Yu, G. Seydoux, M. Krause, F. Gertler and E. Lundquist for reagents used in this study; A. North at the Bio-Imaging Center at Rockefeller University; the *Caenorhabditis* Genetics Center for strains; K. Kemphues and R. Aroian for antibodies; and K. McDonald for use of the Bal-Tec HPM 010 high pressure freezing device and Leica AFS freeze-substitution device at the University of California Berkeley. We thank M. Hatten, M. Hilliard, S. Chalasani, M. Gallegos, G. Hollopeter, J. Gray and F. Kelly for thoughtful comments on the manuscript. This work was funded by a University of California San Francisco Chancellor's Fellowship to C.E.A. and by the Howard Hughes Medical Institute. C.I.B. is an Investigator of the Howard Hughes Medical Institute.

COMPETING INTERESTS STATEMENT

The authors declare that they have no competing financial interests.

Published online at http://www.nature.com/natureneuroscience
Reprints and permissions information is available online at http://npg.nature.com/reprintsandpermissions/

1. Dotti, C.G., Sullivan, C.A. & Banker, G.A. The establishment of polarity by hippocampal neurons in culture. *J. Neurosci.* **8**, 1454–1468 (1988).
2. Inagaki, N. *et al.* CRMP-2 induces axons in cultured hippocampal neurons. *Nat. Neurosci.* **4**, 781–782 (2001).
3. Shi, S.H., Cheng, T., Jan, L.Y. & Jan, Y.N. APC and GSK-3β are involved in mPar3 targeting to the nascent axon and establishment of neuronal polarity. *Curr. Biol.* **14**, 2025–2032 (2004).
4. Kishi, M., Pan, Y.A., Crump, J.G. & Sanes, J.R. Mammalian SAD kinases are required for neuronal polarization. *Science* **307**, 929–932 (2005).
5. Shi, S.H., Jan, L.Y. & Jan, Y.N. Hippocampal neuronal polarity specified by spatially localized mPar3/mPar6 and PI 3-kinase activity. *Cell* **112**, 63–75 (2003).
6. Menager, C., Arimura, N., Fukata, Y. & Kaibuchi, K. PIP3 is involved in neuronal polarization and axon formation. *J. Neurochem.* **89**, 109–118 (2004).
7. da Silva, J.S. & Dotti, C.G. Breaking the neuronal sphere: regulation of the actin cytoskeleton in neuritogenesis. *Nat. Rev. Neurosci.* **3**, 694–704 (2002).
8. Goldberg, J.L. *et al.* Retinal ganglion cells do not extend axons by default: promotion by neurotrophic signaling and electrical activity. *Neuron* **33**, 689–702 (2002).
9. Lefcort, F. & Bentley, D. Organization of cytoskeletal elements and organelles preceding growth cone emergence from an identified neuron *in situ*. *J. Cell Biol.* **108**, 1737–1749 (1989).
10. Halfter, W., Deiss, S. & Schwarz, U. The formation of the axonal pattern in the embryonic avian retina. *J. Comp. Neurol.* **232**, 466–480 (1985).
11. Weiner, O.D. Regulation of cell polarity during eukaryotic chemotaxis: the chemotactic compass. *Curr. Opin. Cell Biol.* **14**, 196–202 (2002).
12. Van Haastert, P.J. & Devreotes, P.N. Chemotaxis: signalling the way forward. *Nat. Rev. Mol. Cell Biol.* **5**, 626–634 (2004).
13. Weiner, O.D. *et al.* A PtdInsP(3)- and Rho GTPase-mediated positive feedback loop regulates neutrophil polarity. *Nat. Cell Biol.* **4**, 509–513 (2002).
14. Hedgecock, E.M., Culotti, J.G. & Hall, D.H. The *unc-5, unc-6*, and *unc-40* genes guide circumferential migrations of pioneer axons and mesodermal cells on the epidermis in *C. elegans*. *Neuron* **4**, 61–85 (1990).
15. Wadsworth, W.G., Bhatt, H. & Hedgecock, E.M. Neuroglia and pioneer neurons express UNC-6 to provide global and local netrin cues for guiding migrations in *C. elegans*. *Neuron* **16**, 35–46 (1996).
16. Serafini, T. *et al.* The netrins define a family of axon outgrowth-promoting proteins homologous to *C. elegans* UNC-6. *Cell* **78**, 409–424 (1994).
17. Hong, K. *et al.* A ligand-gated association between cytoplasmic domains of UNC5 and DCC family receptors converts netrin-induced growth cone attraction to repulsion. *Cell* **97**, 927–941 (1999).

18. Chan, S.S. *et al.* UNC-40, a *C. elegans* homolog of DCC (Deleted in Colorectal Cancer), is required in motile cells responding to UNC-6 netrin cues. *Cell* **87**, 187–195 (1996).
19. Keino-Masu, K. *et al.* Deleted in Colorectal Cancer (DCC) encodes a netrin receptor. *Cell* **87**, 175–185 (1996).
20. Hamelin, M., Zhou, Y., Su, M.W., Scott, I.M. & Culotti, J.G. Expression of the UNC-5 guidance receptor in the touch neurons of *C. elegans* steers their axons dorsally. *Nature* **364**, 327–330 (1993).
21. Desai, C., Garriga, G., McIntire, S.L. & Horvitz, H.R. A genetic pathway for the development of the *Caenorhabditis elegans* HSN motor neurons. *Nature* **336**, 638–646 (1988).
22. Garriga, G., Desai, C. & Horvitz, H.R. Cell interactions control the direction of outgrowth, branching and fasciculation of the HSN axons of *Caenorhabditis elegans*. *Development* **117**, 1071–1087 (1993).
23. Knobel, K.M., Jorgensen, E.M. & Bastiani, M.J. Growth cones stall and collapse during axon outgrowth in *Caenorhabditis elegans*. *Development* **126**, 4489–4498 (1999).
24. Krause, M., Dent, E.W., Bear, J.E., Loureiro, J.J. & Gertler, F.B. Ena/VASP proteins: regulators of the actin cytoskeleton and cell migration. *Annu. Rev. Cell Dev. Biol.* **19**, 541–564 (2003).
25. Gitai, Z., Yu, T.W., Lundquist, E.A., Tessier-Lavigne, M. & Bargmann, C.I. The netrin receptor UNC-40/DCC stimulates axon attraction and outgrowth through enabled and, in parallel, Rac and UNC-115/AbLIM. *Neuron* **37**, 53–65 (2003).
26. Lebrand, C. *et al.* Critical role of Ena/VASP proteins for filopodia formation in neurons and in function downstream of netrin-1. *Neuron* **42**, 37–49 (2004).
27. Manser, J., Roonprapunt, C. & Margolis, B. *C. elegans* cell migration gene *mig-10* shares similarities with a family of SH2 domain proteins and acts cell nonautonomously in excretory canal development. *Dev. Biol.* **184**, 150–164 (1997).
28. Krause, M. *et al.* Lamellipodin, an Ena/VASP ligand, is implicated in the regulation of lamellipodial dynamics. *Dev. Cell* **7**, 571–583 (2004).
29. Stringham, E.G., Dixon, D.K., Jones, D. & Candido, E.P. Temporal and spatial expression patterns of the small heat shock (*hsp16*) genes in transgenic *Caenorhabditis elegans*. *Mol. Biol. Cell* **3**, 221–233 (1992).
30. Gil, E.B., Malone Link, E., Liu, L.X., Johnson, C.D. & Lees, J.A. Regulation of the insulin-like developmental pathway of *Caenorhabditis elegans* by a homolog of the PTEN tumor suppressor gene. *Proc. Natl. Acad. Sci. USA* **96**, 2925–2930 (1999).
31. Morris, J.Z., Tissenbaum, H.A. & Ruvkun, G. A phosphatidylinositol-3-OH kinase family member regulating longevity and diapause in *Caenorhabditis elegans*. *Nature* **382**, 536–539 (1996).
32. Polleux, F., Giger, R.J., Ginty, D.D., Kolodkin, A.L. & Ghosh, A. Patterning of cortical efferent projections by semaphorin-neuropilin interactions. *Science* **282**, 1904–1906 (1998).
33. Lieberam, I., Agalliu, D., Nagasawa, T., Ericson, J. & Jessell, T.M.A. Cxcl12-CXCR4 chemokine signaling pathway defines the initial trajectory of mammalian motor axons. *Neuron* **47**, 667–679 (2005).
34. Gad, J.M., Keeling, S.L., Shu, T., Richards, L.J. & Cooper, H.M. The spatial and temporal expression patterns of netrin receptors, DCC and neogenin, in the developing mouse retina. *Exp. Eye Res.* **70**, 711–722 (2000).
35. Deiner, M.S. *et al.* Netrin-1 and DCC mediate axon guidance locally at the optic disc: loss of function leads to optic nerve hypoplasia. *Neuron* **19**, 575–589 (1997).
36. Hiramoto, M., Hiromi, Y., Giniger, E. & Hotta, Y. The *Drosophila* Netrin receptor Frazzled guides axons by controlling Netrin distribution. *Nature* **406**, 886–889 (2000).
37. Jiang, H., Guo, W., Liang, X. & Rao, Y. Both the establishment and the maintenance of neuronal polarity require active mechanisms: critical roles of GSK-3beta and its upstream regulators. *Cell* **120**, 123–135 (2005).
38. Funamoto, S., Meili, R., Lee, S., Parry, L. & Firtel, R.A. Spatial and temporal regulation of 3-phosphoinositides by PI 3-kinase and PTEN mediates chemotaxis. *Cell* **109**, 611–623 (2002).
39. Iijima, M. & Devreotes, P. Tumor suppressor PTEN mediates sensing of chemoattractant gradients. *Cell* **109**, 599–610 (2002).
40. Ming, G. *et al.* Phospholipase C-gamma and phosphoinositide 3-kinase mediate cytoplasmic signaling in nerve growth cone guidance. *Neuron* **23**, 139–148 (1999).
41. Campbell, D.S. & Holt, C.E. Chemotropic responses of retinal growth cones mediated by rapid local protein synthesis and degradation. *Neuron* **32**, 1013–1026 (2001).
42. Xie, Y. *et al.* Phosphatidylinositol transfer protein-alpha in netrin-1-induced PLC signalling and neurite outgrowth. *Nat. Cell Biol.* **7**, 1124–1132 (2005).
43. Brenner, S. The genetics of *Caenorhabditis elegans*. *Genetics* **77**, 71–94 (1974).
44. Mello, C. & Fire, A. DNA transformation. *Methods Cell Biol.* **48**, 451–482 (1995).
45. Baumeister, R., Liu, Y. & Ruvkun, G. Lineage-specific regulators couple cell lineage asymmetry to the transcription of the *Caenorhabditis elegans* POU gene *unc-86* during neurogenesis. *Genes Dev.* **10**, 1395–1410 (1996).
46. Colavita, A., Krishna, S., Zheng, H., Padgett, R.W. & Culotti, J.G. Pioneer axon guidance by UNC-129, a *C. elegans* TGF-beta. *Science* **281**, 706–709 (1998).
47. Sato, T. A modified method for lead staining of thin sections. *J. Electron Microsc. (Tokyo)* **17**, 158–159 (1968).